Published in final edited form as:
Anal Chem. 2006 June 1; 78(11): 3730–3737.

On-line Sample Preconcentration Using Field-amplified Stacking Injection in Microchip Capillary Electrophoresis

Maojun Gong[†], **Kenneth R. Wehmeyer**[‡], **Patrick A. Limbach**[†], **Francisco Arias**[‡], and **William R. Heineman**[*,†]

†*Department of Chemistry, University of Cincinnati, P.O. Box 210172, Cincinnati, OH 45221-0172, USA*

‡*Procter and Gamble Pharmaceuticals, Health Care Research Center, 8700 Mason-Montgomery Rd, Mason, OH 45040, USA*

Abstract

Previous reports describing sample stacking on microchip capillary electrophoresis (μCE) have regarded the microchip channels as a closed system and treated the bulk flow as in traditional capillary electrophoresis. This work demonstrates that the flows arising from the cross region should be investigated as an open system. It is shown that the pressure-driven flows into or from the branch channels due to bulk velocity mismatch in the main channel should not be neglected but can be used for liquid transportation in the channels. Based on these concepts, a sample preconcentration scheme was developed in a commercially available glass, single-cross chip for μCE. Similar to field-amplified stacking injection in traditional CE, a low conductivity sample buffer plug was introduced into the separation channel immediately before the negatively charged analyte molecules were injected. The detection sensitivity was improved by 94-, 108- and 160-fold for fluorescein-5-isothiocyanate, fluorescein disodium and 5-carboxyfluorescein, respectively, relative to a traditional pinched injection. The calibration curves for fluorescein and 5-carboxyfluorescein demonstrated good linearity in the concentration range (1 to 60 nM) investigated with acceptable reproducibility of migration time and peak height and area ratios (4 to 5% RSD). This preconcentration scheme will be of particular significance to the practical use of μCE in the emerging miniaturized analytical instrumentation.

Microchip capillary electrophoresis (μCE) offers several advantages over traditional capillary electrophoresis (CE), such as reduced sample and reagent consumption, short analysis time, and easy miniaturization of analytical instrumentation.[1] However, the small sample injection volume and short path length available for optical measurements limit the detection schemes of μCE even more than in traditional CE. To improve sensitivity for UV detection, z- or u-shaped optical path and multireflection cells have been employed in μCE.[2,3] Laser induced fluorescence (LIF) detection instead of UV absorbance provides greater sensitivity in both traditional CE and μCE.[4] An additional means of improving detection limits in CE and μCE is to employ sample pretreatment schemes.[5-9] The most widely adapted approaches for on-line sample pretreatment include isotachophoresis,[10,11] sample stacking,[12-14] solid phase extraction,[15-17] and recently sweeping techniques[18-20].

Sample stacking is widely used in traditional CE where detection enhancement factors from 10 to 1000 have been achieved.[6,12-14] In a typical sample stacking approach for anions, the analyte in a low conductivity sample buffer plug (SBP) is injected into the capillary inlet by pressure and then a normal-polarity voltage is applied across the capillary. The sample anions become stacked at the interface between the low- and high-conductivity buffers due to the

[*]Corresponding Author: E-mail: William.Heineman@uc.edu. Tel: (513) 556-9210. Fax: (513) 556-9239.

higher electric field strength in the low-conductivity buffer driving faster migration of the anions relative to the running buffer. However, the laminar flow profile caused by hydraulic pressure on the buffer gradient boundary results in band broadening and loss of resolution.[21] Therefore, the injected SBP length is typically kept to about 10% of the effective capillary length so as to achieve a satisfactory compromise between resolution and enhanced detection sensitivity.[21,22]

To achieve higher detection sensitivity while retaining high resolution, field-amplified stacking injection (FASI) has been developed and used in traditional CE.[23-25] For an anionic analyte, FASI is achieved by introducing a low conductivity solution, such as water, into the capillary from the inlet by pressure. The capillary inlet is then inserted into the sample solution and a reversed-polarity voltage is applied across the capillary. Because of the higher electric field strength in the water plug relative to the running buffer, analyte anions are injected and stacked at the buffer boundary, and simultaneously, the water plug is pumped out of the capillary by the EOF induced by the electric field. This method can afford a sensitivity enhancement of several thousand-fold in traditional CE.[23]

FASI cannot be directly transferred to μCE due to the complexity of the injection and separation channel design. In the simplest μCE design with a single cross, there are four branch channels meeting at the cross region. One set of branch channels comprise the separation capillary (usually channels L_2 and L_4) and the other set of channels comprise the injection capillary (usually channels L_1 and L_3) as shown in Figure 1. The existence of these branch channels creates an open system and makes the practice of sample stacking more complicated. Additionally, the specialized “pinched” injection used with μCE involves multiple voltage steps and demands the application of properly balanced voltages to the reservoirs to avoid diffusion problems.[26] The first reported sample stacking on a single-cross fused quartz microchip was performed by Jacobson and Ramsey[27] with a modified gated injection scheme suitable for negatively charged species with low mobility. Their approach resulted in approximately a 10-fold detection enhancement which was limited by the pressure-driven peak broadening effects.

In recent years, two additional sample stacking schemes on μCE devices have been developed.[28-31] One approach is to inject a large volume of a low conductivity sample solution into the separation channel, or an additional branch channel, and then simultaneously push sample buffer out of the separation channel while stacking the analytes.[28,29] The other approach is to stabilize the conductivity gradient boundaries in the injection region by using an additional branch channel or a porous polymer structure.[30,31] Although these two sample stacking approaches can increase detection sensitivity up to 1000-fold, they are limited by more complicated microchip designs, laborious analytical procedures, a poorly controlled sample injection volume, and difficulty in knowing the locations of preconcentrated analytes of interest.

In this paper, preconcentration of anionic analytes was achieved using a sample buffer plug (SBP) injection followed by FASI with sample buffer removal from the separation channel on a commercially available single-cross glass microchip. The SBP injection and FASI processes were theoretically and experimentally studied and the stacking process was monitored at different locations along the separation channel using anionic and neutral dyes. The optimal injection and separation conditions were developed with FITC, fluorescein disodium salt (FL) and 5-carboxyfluorescein (5-FAM). Finally, the preconcentration scheme was evaluated by examining detection enhancement relative to the standard pinched injection and by constructing calibration curves for FL and 5-FAM using FITC as an internal standard.

EXPERIMENTAL SECTION

Instrumentation

A custom-built μCE system described previously[32,33] was used for all analyses. The analysis was performed on a commercially available (Micralyne Inc., Edmonton, AB, Canada) single-cross glass microchip (Figure 1). The chip has separation and injection channel lengths of 8.50 and 0.80 cm, respectively. Polypropylene reservoirs were attached at the sample reservoir (SR), the sample waste (SW), the buffer reservoir (BR) and the buffer waste (BW) using a two part epoxy. The filtered fluorescence excitation beam (480 ± 20 nm) from a 150-watt xenon lamp was focused onto the microchip channel using the 20x objective of an inverted microscope (Nikon Eclipse TE300, Nikon Corp., Melville, NY, USA). In addition, a CCD-100 camera system (Dage-MTI, Inc., Michigan City, IN) was coupled to the bottom of the microscope and was used together with a video recorder and monitor (Model BWMC, Javelin Systems, Torrace, CA) to record and qualitatively observe flows and analyte movement in the microchip channels.

Chemicals and Reagents

Sodium tetraborate and sodium hydroxide were from Fisher Scientific (Fair Lawn, NJ, USA). FL was from ICN Biomedicals, Inc. (Aurora, OH, USA). BODIPY 530/550 (4,4-difluoro-5,7-diphenyl-4-bora-3a,4a-diaza-*s*-indacene-3-propionic acid, succinimidyl ester), BODIPY 505/515 (4,4-difluoro-1,3,5,7-tetramethyl-4-bora-3a,4a-diaza-*s*-indacene) and FITC isomer I were from Molecular Probes (Eugene, OR, USA). 5-FAM was from Aldrich Chemical Company, Inc. (Milwaukee, WI, USA). All chemicals were used without further treatment.

BODIPY stock solutions were prepared with methanol and all other solutions were prepared with deionized water from a NANOpure system (Sybron Barnstead Corp., Boston, MA, USA). FITC, FL and 5-FAM stock solutions were prepared in water at concentrations of 0.25, 1.0 and 0.44 mM, respectively, and were diluted with water and/or buffer as needed. All solutions used in filling the chip reservoirs were filtered through 0.2-□m syringe filters purchased from Gelman Laboratory, Pall Corp. (Ann Arbor, MI, USA), and the buffer and sample solutions were degassed under vacuum.

μCE Procedures

Chip Conditioning—The channels of the glass chip were conditioned by filling the SR, BR and SW reservoirs sequentially with 1.0 M NaOH for 10 min, deionized water for 10 min, and running buffer for 10 min by applying a vacuum to BW. After the NaOH rinse, all reservoirs were flushed several times with deionized water.

SBP and FASI Process—Following conditioning, an aliquot (30 μL) of running buffer (35.0 mM tetraborate, pH 8.9) was added to BW and SW, 35 μl of running buffer was added to BR, and an aliquot (30 μL) of the analyte in the sample buffer solution (0.50 mM tetraborate, pH 8.3 buffer, unless indicated otherwise) was added to SR. After focusing the detection point of the laser on the main channel, the Labview and Turbochrome programs were manually switched on simultaneously using the voltage setup shown in Figure 1 for the SBP injection/FASI procedure or for a standard pinched injection. All experiments were performed at ambient temperature. All data were processed with Turbochrome software (Version 4.0). Flow videos were captured by the CCD camera and recorded on a video tape, and the flow pictures were selected from the video.

EOF and Electrophoretic Mobility Determination—The EOF and the electrophoretic mobility of FL, FITC and 5-FAM were determined using the same running buffer and sample buffer configuration discussed above in conjunction with a pinched injection program and

BODIPY 530/550 as a neutral marker. The EOF was determined from the migration time of the neutral marker and the electrophoretic mobility of each analyte was then determined.[34]

RESULTS AND DISCUSSION

Description of the SBP and FASI Process

Based on the FASI mechanism used in traditional CE,[23-25] a FASI scheme for stacking in μCE was developed. A four-step procedure was designed as shown in Figure 1 using the voltage configuration shown in each step. First, the low-conductivity sample solution is electroosmotically pumped from SR through the cross region into SW reservoir until the flow reaches a steady state. Then, the voltage setup is switched to the SBP injection state with the application of the voltage between SR and BW resulting in the sample buffer solution being pumped from SR and driven into channels L_2, L_3 and L_4. Next, for FASI, the voltage polarity is reversed from the SBP injection with the voltage being applied between SW and BW resulting in bulk flow into SW through L_3. This bulk flow results in siphoning flows from SR, BR, and BW through L_1, L_2 and L_4, respectively, then the cross region and into SW via L_3. During the FASI step, analyte anions from SR enter the cross region via L_1 and are accelerated and introduced into the separation channel (L_4) due to the applied voltage between SW and BW. The analyte anions are stacked at the interface between the low- and high-conductivity buffers in L_4 and simultaneously most of the low-conductivity buffer is pumped out of L_4 into the SW reservoir. Finally, at the appropriate time, the voltage setup is switched to the separation/dispensing step just before the concentrated sample arrives at the cross, and the analyte zones are separated from one another and detected. Step 1 and Step 4 in this process are the same steps used for a pinched injection in μCE[32] and will not be further considered. The SBP injection (Step 2) and FASI (Step 3) are more complicated and will be discussed in detail below.

Theoretical Considerations for SBP injection

Due to the complexity of the channels in the simple cross microchip used here, the SBP injection and FASI process are more involved than in traditional CE. During the SBP injection step, electrodes for BR and SW are floated, BW is grounded, and SR has a voltage of U_0, thus, the voltage is applied only between SR and BW (Figure 1). Due to the mismatch of EOF velocities produced in L_1 and L_4 as a result of the difference in buffer conductivities, the bulk flow from L_1 (V_1) is divided into three flows into L_2, L_3 and L_4, with bulk velocities of V_2, V_3, and V_4, respectively. Due to the fluid continuity, the solution volume into the cross region is equal to the total volume out as described by Equation 1 where A_1, A_2, A_3, and A_4 are the cross-sectional areas of the four channels.

$$V_1A_1=V_2A_2+V_3A_3+V_4A_4 \quad (1)$$

For simplicity, suppose $A_1 = A_2 = A_3 = A_4$, then

$$V_1=V_2+V_3+V_4 \quad (2)$$

At the moment ($t_0 = 0$) of voltage switching from the loading step to the SBP injection, L_1 is full of sample buffer, L_2 and L_4 are full of running buffer, and L_3 is filled with a mixture of sample buffer and running buffer (Figure 1a-1b). Electric field strengths across L_1 (E_{10}) and L_4 (E_{40}) are described by Equations 3a and 3b,[29] respectively,

$$E_{10}=\frac{\gamma U_0}{\gamma L_1+L_4} \quad (3a)$$

$$E_{40}=\frac{U_0}{\gamma L_1+L_4} \quad (3b)$$

where γ is the conductivity ratio of the running buffer plug (RBP) and the SBP, and U_0 is the applied voltage between SR and BW. After time t_x, a SBP with the length of L_x is injected into L_4 as shown in Figure 1b where x refers to the position of the SBP front in L_4 relative to the cross center. Then, the electric field strengths across the SBP (E_{1x}), which is across $L_1 + L_x$, and across the RBP (E_{4x}), which is across $L_4 - L_x$, are described by Equations 4a and 4b, respectively,

$$E_{1x}=\frac{\gamma U_0}{\gamma (L_1+L_x)+(L_4-L_x)} \tag{4a}$$

$$E_{4x}=\frac{U_0}{\gamma (L_1+L_x)+(L_4-L_x)} \tag{4b}$$

Accordingly, bulk flows (V_{ix}) in each of the branch channels (L_1, L_2, L_3 and L_4) are the vector sums of the local electroosmotic velocities and the pressure-driven velocities in each channel, as expressed in Equations 5a-d.

$$V_{1x}=V_{eo1x}-V_{p1x} \tag{5a}$$

$$V_{2x}=V_{p2x} \tag{5b}$$

$$V_{3x}=V_{p3x} \tag{5c}$$

$$V_{4x}=V_{eo4x}+V_{p4x} \tag{5d}$$

where V_{eo1x} and V_{eo4x} are local EOFs produced in L_1 and L_4, respectively; V_{pix} is the pressure-driven velocity in channel L_i ($i = 1 \sim 4$) . V_{eo1x} can be expressed in terms of the local electroosmotic mobility (μ_{eo1}) and electric field strength (E_{1x}) as shown in Equation 6.

$$V_{eo1x}=\mu_{eo1}E_{1x} \tag{6}$$

Since the L_x part of L_4 is occupied by sample buffer and the rest of L_4 is still full of running buffer, V_{eo4x} is the average of two parts weighted by the ratios as described by Equation 7.[22,35]

$$V_{eo4x}=\left(\frac{L_x}{L_4}\right)\mu_{eo1}E_{1x}+\left(1-\frac{L_x}{L_4}\right)\mu_{eo4}E_{4x} \tag{7}$$

where μ_{eo4} is the electroosmotic mobility in the running buffer.

From Equations 2 and 5:

$$V_{eo1x}-V_{p1x}=V_{p2x}+V_{p3x}+\left(V_{eo4x}+V_{p4x}\right) \tag{8}$$

If it is assumed that the fluid viscosities in the four channels are the same, the chip sits on a horizontal plane and the reservoirs contain the same level of liquid, then the pressure-driven flows will be inversely proportional to their channel lengths as expressed in Equation 9,[36]

$$L_1V_{p1x}=L_2V_{p2x}=L_3V_{p3x}=L_4V_{p4x}=b\Delta P \tag{9}$$

where □P is the pressure drop between the channel end and the cross center, and b is a constant. From the combination of Equations 8 and 9, pressure-driven flow velocities are obtained as shown in Equation 10,[36]

$$V_{pix}=-\frac{\Delta V_{eox}}{L_i\left(\frac{1}{L_1}+\frac{1}{L_2}+\frac{1}{L_3}+\frac{1}{L_4}\right)},\quad i=1\sim 4 \tag{10}$$

where $\Delta V_{eox} = V_{eo1x}\text{-}V_{eo4x}$ is the difference in EOFs in channels L_1 and L_4, and it can be expressed as the function of L_x derived by combining Equations 4, 6 and 7.

$$\Delta V_{eox} = \frac{U_0(\gamma\mu_{eo1} - \mu_{eo4})(1 - L_x/L_4)}{\gamma(L_1 + L_x) + (L_4 - L_x)} \tag{11}$$

Generally, $\gamma\mu_{eo1}$ is much larger than μ_{eo4} when the two buffers have similar pH values and as a result ΔV_{eox} is positive, and the SBP in channel L_1 produces a pressure to the solution plugs in the branch channels connected to the cross region.[36-38]

For a specific model system on a microchip, the applied voltage (U_0) and the buffer conductivity ratio (γ) are selected and kept constant assuming that electrolysis, ion diffusion and liquid convection are negligible. In our case, $U_0 = 1000$ V and $\gamma = 70$ (ratio of the tetraborate concentrations of the running buffer and the sample buffer); $L_1 = L_3 = 0.40$ cm, $L_2 = 0.50$ cm and $L_4 = 8.00$ cm. The electroosmotic mobilities for 0.50- and 35.0-mM tetraborate buffer are 6.18 and 4.06 ($\times 10^{-4}$ cm^2/Vs) , respectively. Substituting these values into Equation 11, ΔV_{eox} can be expressed as Equation 12. The bulk velocities in the four channels (Equations 5a-d) are as presented in Equations 13a-d. The corresponding relationship diagrams for ΔV_{eox} and bulk channel velocities versus L_x are shown in Figure 2.

$$\Delta V_{eox} = \frac{42.9 - 5.4L_x}{36.0 + 69.0L_x} \tag{12}$$

$$V_{1x} = \frac{28.2 + 1.9L_x}{36.0 + 69.0L_x} \tag{13a}$$

$$V_{2x} = \frac{12.0 - 1.5L_x}{36.0 + 69.0L_x} \tag{13b}$$

$$V_{3x} = \frac{15.0 - 1.9L_x}{36.0 + 69.0L_x} \tag{13c}$$

$$V_{4x} = \frac{1.2 + 5.3L_x}{36.0 + 69.0L_x} \tag{13d}$$

The trendlines in Figure 2 show that ΔV_{eox} is decreasing rapidly as the SBP is injected L_4. Accordingly, the bulk flow velocities in channel L_1, L_2, and L_3 are decreasing. However, the bulk flow velocity in L_4 is still gently increasing, which is caused by the higher electroosmotic flow velocity of the low conductivity sample buffer injected into L_4. It also shows that the bulk velocities in L_2 and L_3 (V_{2x} and V_{3x}) are significantly higher than that in L_4 (V_{4x}) when L_x is short. It is easy to understand that the pressure-driven flow velocity in L_4 is significantly lower than in L_2 and L_3 since the lengths of these two channels, 0.50 and 0.40 cm, respectively, are significantly shorter than L_4 (8.00 cm). In addition, the electroosmotic velocity produced in L_4 is relatively low due to the high conductivity of the running buffer relative to the sample buffer.

The bulk flows from the cross region during the SBP injection were monitored with a neutral dye, BODIPY 505/515. As can be seen in Figure 3a, as soon as the SBP injection voltage was switched on, the SBP was introduced into L_4 as well as L_2 and L_3. After a short time of 100 ms, the SBP length in L_4 is approximately four times shorter than that in L_2 as predicted by the relative bulk flow velocities described in Figure 2. As time progresses, the neutral dye migrates further into channels L_2 and L_4. It should be noted channel L_3 is filled with the neutral dye at all times during the SBP injection since it was introduced into this channel during the sample loading step (Figure 1a). Under the applied voltage, the negatively charged analyte in the

sample buffer has an electrophoretic velocity ($V_{ep} = \mu_{ep}E$)[35] and is in a direction opposite of the EOF. In the two-buffer system, the analytes are in low-conductivity buffer with much higher local electric field strength than the high-conductivity buffer. The electrophoretic velocity, V_{ep}, of the analyte anions can be expressed as in Equation 14.

$$V_{ep}=\frac{\mu_{ep}\gamma U_0}{\gamma(L_1+L_x)+(L_4-L_x)} \quad (14)$$

By inserting the values of all the variables (L_1, L_4, □, U_0 and $\mu_{ep} = 1.46 \times cm^2/Vs$ of FL in 0.50 mM tetraborate) into Equation 14, the electrophoretic velocity of FL anions (V_{epFL}) in the low-conductivity buffer using 35.0 mM sodium tetraborate as the high-conductivity buffer is shown in Equation 15.

$$V_{epFL}=\frac{10.2}{36.0+69.0L_x} \quad (15)$$

The apparent velocity of the FL anions in the SBP of L_x is the vector sum of the bulk flow V_{4x} (Equation 13d) and the electrophoretic velocity V_{epFL} (Equation 15). When $V_{epFL} \geq V_{4x}$, i.e. $L_x \leq 1.70$ cm, the FL anions are moving toward the channel cross and are rejected from entering the separation channel. This effect is confirmed by monitoring the FL anions during the SBP injection process (Figure 3b). It can also be seen in Figure 3b that FL anions do not enter L_3 but do enter L_2. The FL anions were pulled into the cross region, close to L_4, by the electric field and then a portion of the FL anions are pushed from the cross region into L_2 by the pressure-driven flow (V_{2x}) into this channel. It is noted that the application of the potentials generate a curved electrical field around the corner of the cross which can be visualized from the movement of the FL anions in the cross region. Thus, the SBP step serves as a means of introducing low-conductivity buffer into a portion of L_4 to aid stacking during the FASI step which is discussed below.

Field-amplified Stacking Injection

During the FASI process, a voltage U_0 is applied at BW, while SW is grounded, SR is floated and a voltage, U_1 (0.26 KV), is applied at BR as indicated in Figure 1c. The FASI process in many respects will be just the reverse of the SBP injection step since L_1 and L_3 have the same dimensions and assuming that the buffer in L_3 approximates that in L_1 by the time the FASI step is initiated. The application of the reversed-polarity voltage between BW and SW creates an EOF moving between L_4 and L_3; however, the bulk flow in L_3 (V_{3x}) will be significantly larger than the bulk flow in L_4 (V_{4x}). Thus the bulk flow in L_3 will induce a siphoning (pulling) effect in the cross region and will cause siphoning flows in L_1 (V_{1x}), L_2 (V_{2x}) and L_4 (V_{4x}) in a manner similar to the pressure-induced flows in the channels during the SBP injection. In addition, the small voltage applied to BR will also generate an electric field strength in L_2 that is in the direction of BR at the beginning of the FASI step and reverses as the FASI proceeds. The magnitude of the bulk velocity in channel L_3 during FASI will be similar to what was obtained in channel L_1 during the SBP injection (Equations 3a and 13a). The electrophoretic velocity of FL anions (V_{epFL}) is as expressed in Equations 14 and 15 and is in the opposite direction of the bulk flows in L_3 and L_4. For the model system discussed in the SBP injection process, the apparent velocity of FL anions in channel L_3 during the FASI process is in the direction of the SW reservoir ($V_{3x} > V_{epFL}$), i.e. the bulk flow in channel L_3 carries FL anions into the SW reservoir without being injected into the separation channel L_4 for stacking. However, the electrical field distribution during the FASI processes, similar to the SBP injection, produces curved potential lines in the cross regions due to the turns of the channels. The FL anions moving into the cross region from SR during the FASI process are pulled into the separation channel by the electrical field and are electrophoretically drawn toward the BW reservoir and end up stacking at the interface between the low/high-conductivity buffers in L_4. Simultaneously, the low conductivity sample buffer introduced during the SBP injection

is pushed out of L_4 and into L_3 by the bulk flow in L_4. Thus, the FL anions driven into L_4 from SR, are stacked in L_4 at the discontinuous buffer interface, and the buffer interface is simultaneously swept back toward the cross region.

The FASI process was visualized by separately using a neutral (BODIPY 505/515) and an anionic (FL) dyes. As a result of the SBP injection, the neutral dye is essentially uniformly distributed in the cross region and channels that are in the field of view at the initiation of the FASI process (Figure 4a). However, as time progresses the neutral dye can be seen to clear from L_4 as a result of the induced siphoning flow and adopts a defined profile in L_3 which is the result of the curved electrical field profile in the cross region (Figure 4a). Similarly, at the initiation of the FASI process, the FL anions are relatively uniformly distributed in the channels visible in the field of view (Figure 4b). However, as time progresses the FL anions are cleared from L_3 and L_2 as a result of the bulk flow induced in L_3 and the corresponding siphoning flow induced in L_2. In L_4, a bright zone of stacked FL anions are visible near the cross region at the end of the FASI process (Figure 4b). The stacked FL anions in L_4 originate from a continuous flow of FL anions being pulled from SR into the cross region by a combination of the siphoning flow induced in L_1 and the curved electric field existing in the cross region. The induced flow from L_1 continues to provide FL anions for injection until the dispensing voltage setup is switched on. The injected amount of FL anions is related to the volume of sample solution from channel L_1 flowing into the cross region. Thus the rate of introduction of FL anions into the cross region is controlled by the siphoning flow in L_1 which can be controlled by adjusting the relative length of each channel. Significantly, a higher concentration enhancement will be achieved by reducing the length of L_1.

Optimization of SBP Injection Length

The SBP length was found to be crucial for the final detection enhancement obtained in the overall process. The optimum SBP length was determined by varying the combination of the SBP injection time (Figure 1b) and the FASI duration (Figure 1c) while holding the other steps (Figures 1a and 1d) constant and monitoring the resulting signal for FITC and FL (Figure 5). It can be seen that if the SBP injection time is too short or too long, that is the SBP is too small or too long, a lower peak signal was obtained for both FITC and FL. If the SBP injection is too short, the amount of time available for stacking analyte anions from the siphoning-induced flow from L_1 is reduced and correspondingly the signal enhancement is reduced. If the SBP plug is too long, several effects will combine to reduce the signal enhancement. Under ideal conditions with no diffusion and convection between buffers, longer SBP (L_x) should not adversely affect the signal because the amount of analyte anions injected into L_4 is a result of the siphoning flow induced in L_1. However, the siphoning flow from L_2 contains high-conductivity running buffer which will mix with the low conductivity sample buffer already present in channel L_3. The increased conductivity of the buffer in L_3 reduces the bulk flow in L_3 and correspondingly reduces the siphoning flow from L_1 and results in a decreased amount of anions being injected into L_4 for stacking. In addition, a longer SBP plug needs a longer SBP injection time which will cause more significant diffusion and mixing of the discontinuous buffer system leading to peak broadening. In these experiments, a SBP injection time of 15 s was found to be optimal.

Process Monitoring

In Figure 6, the SBP injection and the FASI processes for FL anions were examined in L_4 at several locations displaced from the cross region. In Figure 6a, the monitoring was done at 50 μm from the cross region using a 30-s loading period (Figure 1a), followed by a 15-s SBP injection (Figure 1b) and an extended FASI period (60 s, Figure 1c) to allow the visualization of the stacked peak moving into the cross region. It can be seen that a small amount of analyte was introduced into L_4 during the loading process but none was introduced during the 15-s

SBP injection time (30 s to 45 s in Figure 6a), while at the beginning of the FASI process (45 s to 52 s on Figure 6a) FL anions are injected into L_4 (as shown in Figure 4b) and finally the stacked FL anions move past the detection point as indicated by the large peak observed from 50 to 70 s in Figure 6a. The FASI process and the dispensing step were examined at several points along the separation channel, again relative to the cross region, in Figure 6b using the standard voltage program (Figure 1). When monitoring at distances of 2, 4 and 6 mm from the cross, two peaks are seen in the electropherogram. The first peak is due to the stacked FL anions as they are swept back past the monitoring point toward the cross region during the FASI step. The second peak is due to the FL anions as they migrate down the separation channel during the dispensing/separation step. When the detection site was 8 mm from the cross, the first peak was not observed because the conductivity interface possibly failed to reach this point during the 15-s SBP injection. Thus, the SBP length injected is between 6 and 8 mm. It was found that 15 s for SBP injection and 13 s for FASI produced optimal stacking results, and they were used for all other experiments.

Conductivity Ratio Effect

Sample stacking is based on the uneven distribution of the electric field in a discontinuous buffer system leading to the rapid movement of charged species in the low-conductivity matrix with immediate slowing down at the boundary of the two buffers. Theoretically, the concentration enhancement should be proportional to the conductivity ratio of the two buffers.[27] However, due to pressure-driven laminar flow and diffusion/convection mixing of the discontinuous buffers, the interface and the conductivity ratio of the two buffers are rarely kept ideal in practical operations; thus, the concentration enhancement generally is lower than expected. A conductivity ratio of ten has been found to produce optimal enhancement and to maintain resolution in normal stacking mode.[21,27] The conductivity ratio of the running buffer to SBP was investigated by monitoring the fluorescence response for FL anions at 50 μm from the cross region in the separation channel (Figure 7) using the SBP/FASI voltage program given in Figure 1. When the SBP had the same conductivity as that of the running buffer (γ = 1), no sample stacking was obtained. The signal enhancement increased as the conductivity ratio increased. Water or an organic solvent is the best choice for the highest enrichment; however, it is difficult to keep the SBP from being contaminated during operation due to the open flow nature of single cross microchip. Thus, 0.50 mM tetraborate was chosen as a reasonable compromise for all experiments.

Detection Enhancement

The optimized SBP injection and FASI process was compared to the standard pinched injection (steps 1 and 4 in Figure 1) to examine the achievable detection enhancement. For the SBP/FASI process, the sample solution of FITC, FL and 5-FAM at 50 nM each was prepared in 0.50 mM tetraborate buffer (pH 8.3), while for the standard pinched injection process FITC, FL or 5-FAM at 400 nM each were dissolved in 35.0 mM tetraborate, pH 8.9. The detection enhancement was calculated by comparing the peak height for each analyte of the 50 nM sample solution obtained from the SBP injection/FASI process with the peak height for each analyte of the 400 nM solution obtained by the pinched injection. The detection enhancements are 94-, 108- and 160-fold for FITC, FL and 5-FAM, respectively. Their corresponding limits of Detection (LODs), defined at 3x the signal-to-noise (S/N), are lowered by 100-, 110- and 170-fold, The enhancements for FITC, FL and 5-FAM are different and follow their electrophoretic mobilities with 5-FAM giving the largest and FITC giving the smallest enhancements. Thus, it can be concluded that the enhancement is more advantageous for species with high electrophoretic mobilities in this stacking injection scheme.

Calibration Curves

FL and 5-FAM were used to evaluate the concentration linearity of the SBP injection/FASI process. The concentration ranges for the standards were from 1 nM to 64 nM for FL and from 2 nM to 60 nM for 5-FAM, while the concentration of FITC was kept constant at 15 nM to serve as the internal standard. Both the peak height and peak area ratios demonstrated good linearity for both analytes over the concentration ranges investigated. The equations and the correlation coefficients for the peak height ratios are $y = 0.151x + 0.08$, $R^2 = 0.998$ and $y = 0.073x + 0.026$, $R^2 = 0.999$ for FL and 5-FAM, respectively. The equations and the correlation coefficients for the peak area ratios are $y = 0.175x + 0.071$, $R^2 = 0.999$ and $y = 0.126x + 0.073$, $R^2 = 0.999$ for FL and 5-FAM, respectively. The percent RSD ($n = 4$) of the migration time, peak height and peak area are approximately 4, 5 and 5%, respectively, for FL and 5-FAM. The peak height and peak area ratios relative to FITC were each less than 4% for both FL and 5-FAM.

CONCLUSIONS

The flows and analyte movements in μCE are complicated processes due to the open communication between the various channels, especially when involving a discontinuous buffer system. The valveless branched channels need to be taken into account when a discontinuous buffer system is involved, and the pressure-driven/-induced pumping effect in the channel cross region can be utilized to achieve liquid transport and ion discrimination. The theoretical and experimental investigations demonstrated that FASI is a robust and useful on-line preconcentration method on commercially available microchips. Although this scheme just produced around 100-fold detection enhancements for the analytes used, the detection enhancement can be further improved by employing different chip designs. This preconcentration scheme will enlighten the development of the on-line sample preconcentration in μCE and will be of particular significance to the detection capability in the emerging miniaturized analytical instrumentation.

ACKNOWLEDGEMENT

Thanks to Dr. James J. Bao (School of Pharmaceutical Science and Technology, Tianjin University, China) for his review of the manuscript. Financial support was provided by the NIH (GM 69547) and the University of Cincinnati.

REFERENCES

(1). Dolnik V, Liu S, Jovanovich S. Electrophoresis 2000;21:41–45. [PubMed: 10634469]
(2). Liang Z, Chiem N, Ocvirk G, Tang T, Fluri K, Harrison DJ. Anal. Chem 1996;68:1040–1046.
(3). Salimi-Moosavi H, Jiang Y, Lester L, Mckinnon G, Harrison DJ. Electrophoresis 2000;21:1291–1299. [PubMed: 10826672]
(4). Albin M, Grossman PD, Moring SE. Anal. Chem 1993;65:489A.
(5). MOsbourn D, Weiss DJ, Lunte CE. Electrophoresis 2000;21:2768–2779. [PubMed: 11001283]
(6). Shihabi ZK. J. Chromatogr. A 2000;902:107–117. [PubMed: 11192150]
(7). Quirino JP, Terabe S. J. of Chromatogr. A 2000;902:119–135. [PubMed: 11192151]
(8). Beckers JL, Bocek P. Electrophoresis 2000;21:2747–2767. [PubMed: 11001282]
(9). Chien R. Electrophoresis 2003;24:486–497. [PubMed: 12569539]
(10). Shihabi ZK. Electrophoresis 2002;23:1612–1617. [PubMed: 12179979]
(11). Xu ZQ, Hirokawa T, Nishine T, Arai A. J. Chromatogr. A 2003;990:53–61. [PubMed: 12685583]
(12). Beard NP, Zhang CX, deMello AJ. Electrophoresis 2003;24:732–739. [PubMed: 12601745]
(13). Maeso N, Cifuentes A, Coral Barbas C. J. Chromatogr. B 2004;809:147–152.
(14). Chen ZL, Naidu R. J. Chromatogr. A 2004;1023:151–157. [PubMed: 14760859]
(15). Strausbauch M, Landers JP, Wettstein PJ. Anal. Chem 1996;68:306–314. [PubMed: 9027238]

(16). Li J, Thibault P, Martin A, Richards JC, Wakarchuk WW, van der Wilp W. J. Chromatogr. A 1998;817:325–336. [PubMed: 9764503]

(17). Zhang P, Xu G, Xiong J, Zheng Y, Shi X, Yang Q, Wei F. J. Sep. Sci 2003;26:1527–1532.

(18). Quirino JP, Terabe S. Science 1998;282:465–468. [PubMed: 9774271]Sera Y, Matsubara N, Otsuka K, Terabe S. Electrophoresis 2001;22:3509–3513. [PubMed: 11669534]66

(19). Monton MRN, Quirino JP, Otsuka K, Terabe S. J. Chromatogr. A 2001;939:99–108. [PubMed: 11806550]

(20). Wu CH, Chen MC, Su AK, Shu PY, Chou SH. J. Chromatogr. B 2003;785:317–325.

(21). Burgi DS, Chien R. Anal. Chem 1991;63:2042–2047.

(22). Chien R, Helmer JC. Anal. Chem 1991;63:1354–1361.

(23). Martinez D, Borrull F, Clull M. J. Chromatogr. A 1997:185–193.

(24). Zhu L, Lee HK. Anal. Chem 2001;73:3065–3072. [PubMed: 11467555]

(25). Zhu L, Tham SY, Yap AUJ, Lee HK. J. Sep. Sci 2002;25:328–332.

(26). Alarie JP, Jacobson SC, Culbertson CT, Ramsey JM. Electrophoresis 2000;21:100–106. [PubMed: 10634475]

(27). Jacobson SC, Ramsey JM. Electrophoresis 1995;16:481–486. [PubMed: 7588514]

(28). Lichtenberg J, Verpoorte E, de Rooij NF. Electrophoresis 2001;22:258–271. [PubMed: 11288893]

(29). Li J, Wang C, Kelly JF, Harrison DJ, Thibault P. Electrophoresis 2000;21:198–210. [PubMed: 10634488]

(30). Yang H, Chien R. J. Chromatogr. A 2001;924:155–163. [PubMed: 11521862]

(31). Jung B, Bharadwaj R, Santiago JG. Electrophoresis 2003;24:3476–3483. [PubMed: 14595694]

(32). Starkey DE, Han A, Bao JJ, Ahn CH, Wehmeyer KR, Prenger MC, Halsall HB, Heineman WR. J. Chromatogr. B 2001;762:33–41.

(33). Starkey DE, Abdelaziez Y, Ahn CH, Tu J, Anderson L, Wehmeyer KR, Izzo NJ, Carr AN, Peters KG, Bao JJ, Halsall HB, Heineman WR. Anal. Biochem 2003;316:181–191. [PubMed: 12711339]

(34). Williams BA, Vigh G. Anal. Chem 1996;68:1174–1180.

(35). Chien R, Burgi DS. Anal. Chem 1992;64:489A–496A.

(36). Culbertson CT, Ramsey RS, Ramsey JM. Anal. Chem 2000;72:2285–2291. [PubMed: 10845376]

(37). Ramsey RS, Ramsey JM. Anal. Chem 1997;69:1174–1178.

(38). Chien R, Bousse L. Electrophoresis 2002;23:1862–1869. [PubMed: 12116129]

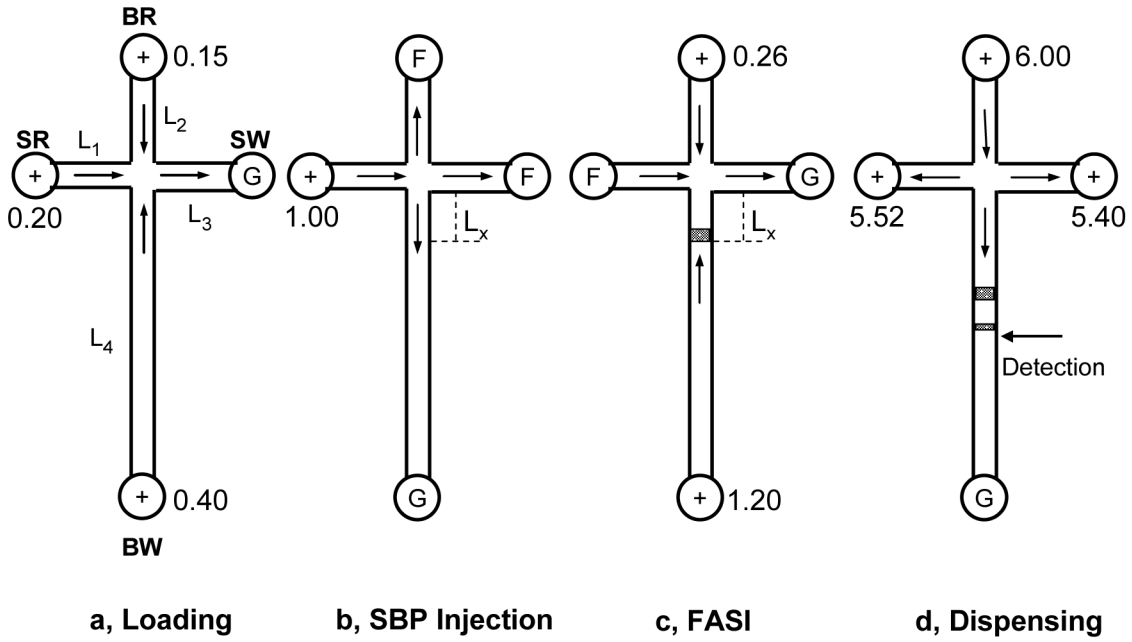

Figure 1.

Four-step procedure for sample buffer plug (SBP) injection/field-amplified stacking injection (FASI). Step 1 (Loading): the low-conductivity sample solution is pumped through the channel cross into the SW until the flow reaches a steady state; Step 2 (SBP Injection): a SBP is pumped into the separation channel, simultaneously, the sample buffer solution also flows into channel L_2 and L_3, and accumulates in the BR and BW reservoirs, respectively; Step 3 (FASI): charged analytes from channel L_1 are introduced into the separation channel and simultaneously the SBP is pumped backwards into SW and Step 4 (Dispensing/Separation): analyte zones are separated from one another and are detected with LIF. SR = Sample Reservoir; SW = Sample Waste reservoir; BR = Buffer Reservoir; BW = Buffer Waste reservoir; F = Floated; G = Grounded. Unit of voltages beside each reservoir is kilovolt (KV). $L_{1\sim4}$ are lengths of four channels from the cross center. L_x is the sample buffer plug length in channel L_4. Arrows indicate bulk flow directions. Size is not proportional to the real dimensions.

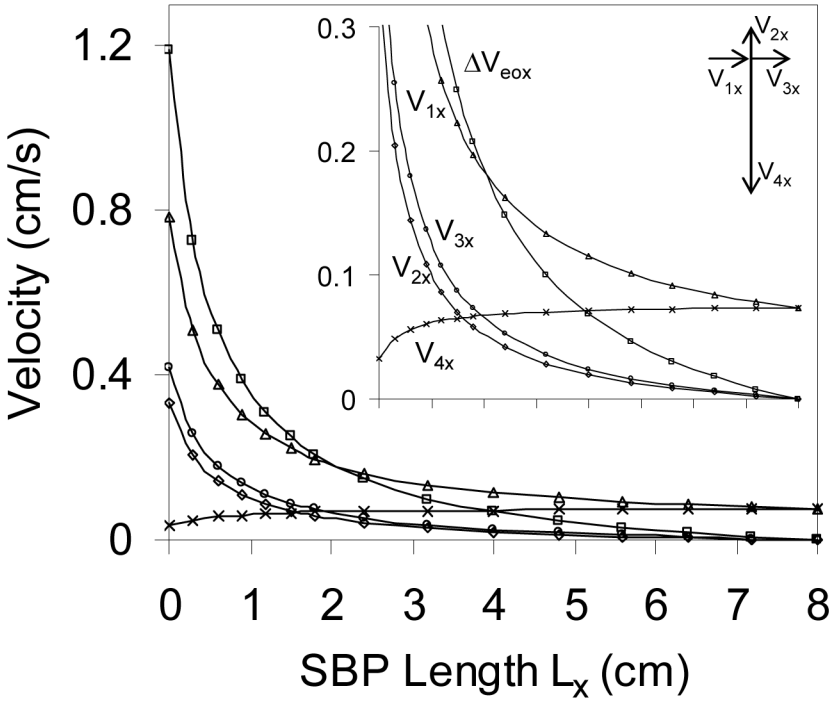

Figure 2.

Plot of the calculated bulk flow velocities in four channels versus SBP length in channel L_4 during SBP injection. Calculations based on Equation 12 and Equations 13a-13d under a voltage of 1000 V, channel lengths of $L_1 = L_3 = 0.40$ cm, $L_2 = 0.50$ cm and $L_4 = 8.00$ cm and a conductivity ratio □ = 70. V_{1x}, V_{2x}, V_{3x}, and V_{4x} are the bulk velocities in channel L_1, L_2, L_3 and L_4, respectively, and □V_{eo} is the EOF velocity difference in channels L_1 and L_4.

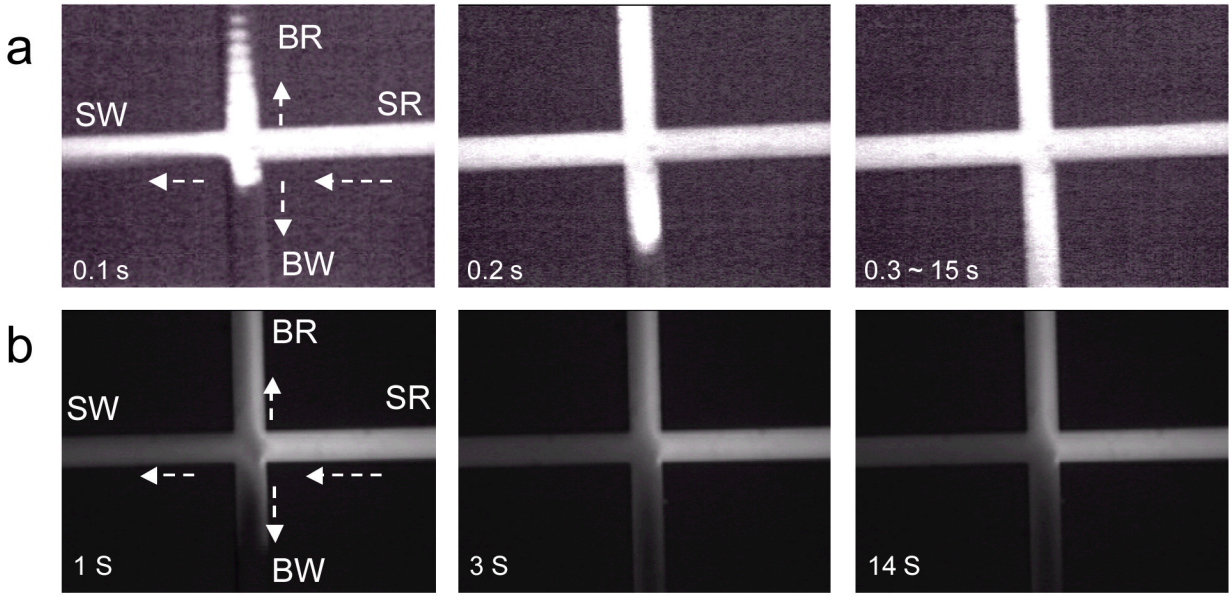

Figure 3.
Pictures of SBP injection process in the near channel cross region. (a) monitored with BODIPY 505/515 (3.0 mM in 60% methanol containing 1.0 mM tetraborate) and (b) monitored with FL (200 μM in 0.50 mM tetraborate buffer). The arrows indicate bulk flow directions.

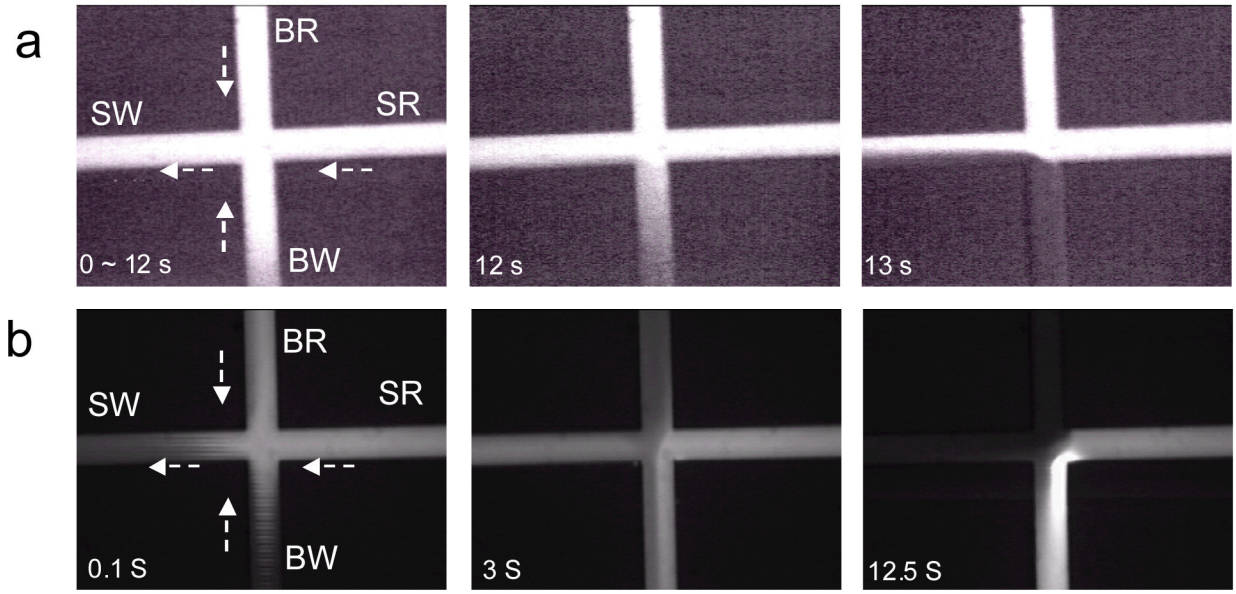

Figure 4.

Pictures of FASI process in the near channel cross region. (a) monitored with BODIPY 505/515 (3.0 mM in 60% methanol containing 1.0 mM tetraborate) and (b) monitored with FL (200 μM in 0.50 mM tetraborate buffer). The arrows indicate bulk flow directions.

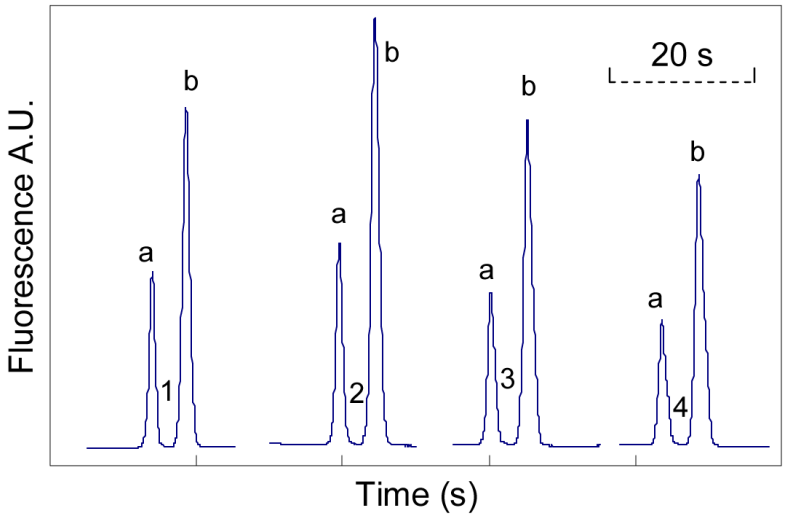

Figure 5.

SBP length effect on signal enhancement expressed in terms of SBP injection time for a sample containing 50 nM FITC and 100 nM FL, detected at 4.0 cm. Conditions 1, 2, 3 and 4 were with 10-, 15-, 20- and 25-s SBP injection time, respectively; the FASI duration was 2 s less than the corresponding SBP injection time. Peak a is FITC and peak b is FL.

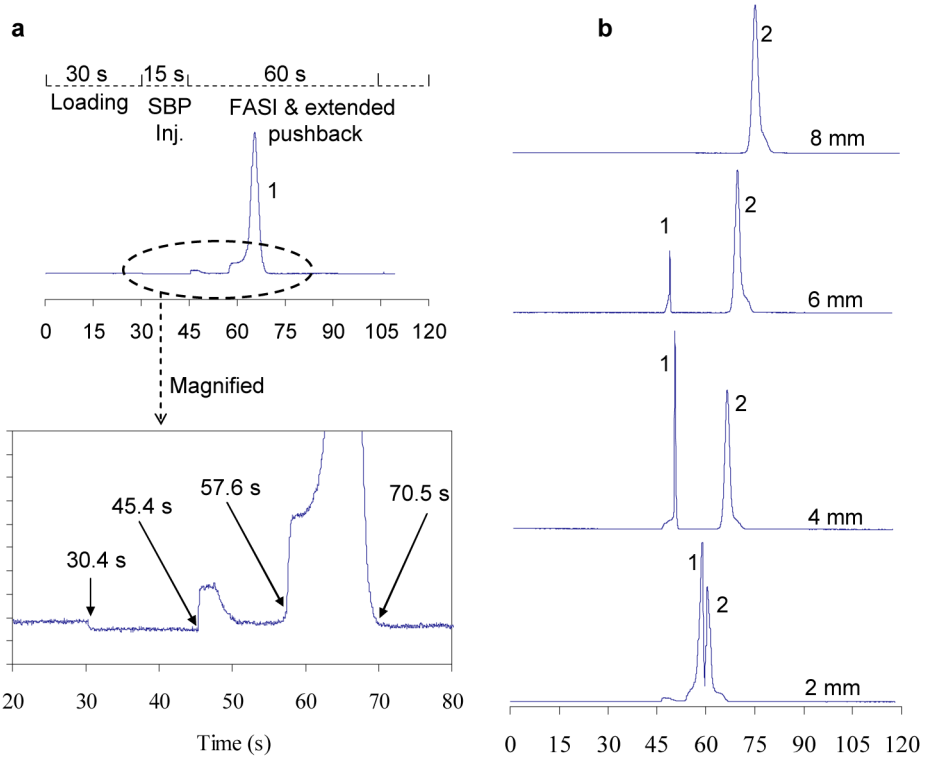

Figure 6.

Stacking processes monitored with 100 nM FL. (a) Monitored at 50 μm in L_4 from the cross region using conditions given in Figure 1 with the exception that the FASI period was extended to 60 s; the lower electropherogram is an expanded view of the upper one. (b) Monitored at different locations along the separation channel with the conditions given in Figure 1. Peaks 1 and 2 are the stacked analytes during FASI and dispensing processes, respectively.

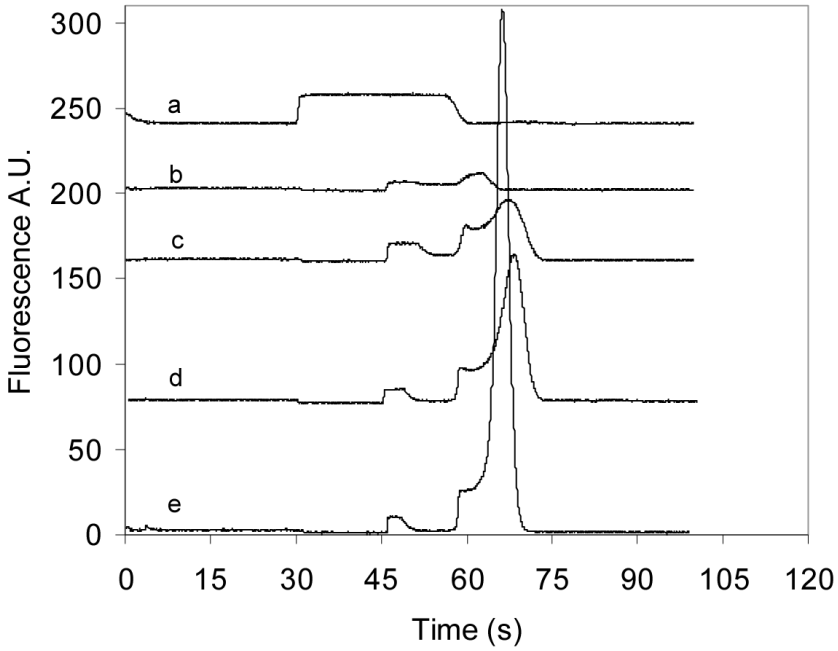

Figure 7.
Conductivity ratio effect of running buffer and sample buffer monitored in L_4 at 50 μm from the cross. 100 nM FL in: a, 35.0 mM; b, 20.0 mM; c, 10.0 mM; d, 3.5 mM; and e, 0.50 mM tetraborate. Running buffer 35.0 mM tetraborate.